

# Numerical Analysis of an Industrial-Scale Steam Methane Reformer

Chun-Lang Yeh \*

Department of Marine Engineering, National Taiwan Ocean University, Keelung, Taiwan

Received 02 March 2018; received in revised form 24 June 2018; accepted 29 July 2018

## Abstract

A steam reformer of a hydrogen plant is a device that supplies heat to convert the natural gas or liquid petroleum gas into hydrogen via catalysis. It has been often used in the petrochemical industry to produce hydrogen. Control of the catalyst tube temperature is a fundamental demand of the reformer design because the tube temperature must be maintained within a range that the tube has minor damage and the catalysts have a high activity to convert the natural gas or liquid petroleum gas into hydrogen. In this research, the effect of the burner on/off manners on the catalyst tube temperature and the hydrogen yield of an industrial-scale side-fired steam methane reformer is investigated. The aim is to seek a feasible burner on/off manner that has acceptable catalyst tube temperature and hydrogen yield, so as to improve the performance and service life of a steam methane reformer. It is found that when one group of burners is turned off, the outer surface temperatures of the tubes are decreased by about 94 °C in average, the inner surface temperatures are decreased by about 54 °C in average, and the hydrogen yields are decreased by about 4%. When two groups of burners are turned off, the outer surface temperatures of the tubes are decreased by about 175 °C in average, the inner surface temperatures are decreased by about 106 °C in average, and the hydrogen yields are decreased by about 7.9%. When three groups of burners are turned off, the outer surface temperatures of the tubes are decreased by about 251 °C in average, the inner surface temperatures are decreased by about 151 °C in average, and the hydrogen yields are decreased by about 11.4%. The catalyst tube temperatures and the hydrogen yields reduce to a greater extent in regions where burners are turned off. When the central groups of burners are turned off, the tube temperatures and the hydrogen yields have greater reductions. On the other hand, when the rear groups of burners are turned off, the tube temperatures and the hydrogen yields have lower reductions.

**Keywords:** hydrogen, steam methane reformer, catalyst tube, burner operation

## 1. Introduction

A steam reformer of a hydrogen plant is a device that supplies heat to convert the natural gas or liquid petroleum gas into hydrogen via catalysts. Hydrogen is an important material for petroleum refineries. It converts crude oil into products with high economic value, e.g., gasoline, jet fuel, and diesel. Hydrogen can be produced by a number of ways, e.g., electrolysis, Steam Methane Reforming (SMR), partial oxidation reforming, nuclear energy, etc. [1,2] Among these ways, SMR is the most common commercial method of industrial hydrogen production. SMR reaction mainly includes the following three chemical equations:



\* Corresponding author. E-mail address: clyeh@nfu.edu.tw

The first (SMR) and the third reactions are endothermic, the second reaction (Water-Gas Shift (WGS)) is exothermic, and the overall reaction is endothermic.

The combustion process in a reformer provides heat to maintain the reforming reaction in a catalyst tube. Control of the catalyst tube temperature is a fundamental demand of the reformer design because the tube temperature must be maintained within a range that the tube has minor damage and the catalysts have a high activity to convert the natural gas or liquid petroleum gas into hydrogen. When a steam reformer is operating, the catalyst tubes are subjected to stresses close to the ultimate stress of the tube material. This leads to an acceleration of the creep damage. Safety, reliability, and efficiency are the basic requirements of the reformer operation. The catalyst tube should have uniform heat distribution to extend the tube service life. However, the heat distribution in a reformer is practically non-uniform. In addition, maldistribution of the flue gas and fuel gas may result in flame impingement on the catalyst tubes and lead to localized hot spots and high tube wall temperature. These factors may shorten tube life.

Owing to the rapid development in computer science and technology, as well as the improvements in physical models and numerical methods, Computational Fluid Dynamics (CFD) is widely used in analyzing systems involving heat transfer, fluid flow, and chemical reactions. CFD is also used to simulate systems that cannot be measured easily or simulated experimentally. In recent years, there have been a lot of SMR researches using CFD. Tran et al. [3] developed a CFD model of an industrial-scale steam methane reformer. The authors pointed out that the reformer CFD model can be considered an adequate representation of the on-line reformer and can be used to determine the risk of operating the online reformer at unexplored and potentially more beneficial operating conditions. Di Carlo et al. [4] investigated numerically a pilot scale bubbling fluidized bed SE-SMR (Sorption Enhanced Steam Methane Reforming) reactor by means of a two-dimensional CFD approach. The numerical results show quantitatively the positive influence of carbon dioxide sorption on the reforming process at different operating conditions, specifically the enhancement of hydrogen yield and reduction of methane residual concentration in the reactor outlet stream. Lao et al. [5] developed a CFD model of an industrial-scale reforming tube using ANSYS Fluent with realistic geometry characteristics to simulate the transport and chemical reaction phenomena with the approximate representation of the catalyst packing. The authors analyzed the real-time regulation of the hydrogen production by choosing the outer wall temperature profile of the reforming tube and the hydrogen concentration at the outlet as the manipulated input and controlled output, respectively. Mokheimer et al. [6] presented modeling and simulations of the SMR process. The model was applied to study the effect of different operating parameters on the steam and methane conversion. The results showed that increasing the conversion thermodynamic limits with the decrease of the pressure results in a need for long reformers so as to achieve the associated fuel reforming thermodynamics limit. It is also shown that not only increasing the steam to methane molar ratio is favorable for higher methane conversion but the way the ratio is changed also matters to a considerable extent. Ni [7] developed a 2D heat and mass transfer model to investigate the fundamental transport phenomenon and chemical reaction kinetics in a compact reformer for hydrogen production by SMR. Parametric simulations were performed to examine the effects of permeability, gas velocity, temperature, and rate of heat supply on the reformer performance. It was found that the reaction rates of SMR and WGS are the highest at the inlet but decrease significantly along with the reformer. Increasing the operating temperature raises the reaction rates at the inlet but shows very small influence downstream. Ebrahimi et al. [8] applied a three-dimensional zone method to an industrial fired heater of the SMR reactor. The effect of emissivity, extinction coefficient, heat release pattern and flame angle on the performance of the fired heater are presented. It was found that decreasing the extinction coefficients of combustion gases by 25% caused a 2.6% rise in the temperature of heat sink surfaces. Seo et al. [9] investigated numerically a compact SMR system integrated with a WGS reactor. Heat transfer to the catalyst beds and the catalytic reactions in the SMR and WGS catalyst beds were investigated. The effects of the cooling heat flux at the outside wall of the system and steam-to-carbon ratio were also examined. It was found that as the cooling heat flux increases, both the methane conversion and carbon monoxide content are reduced in the SMR bed and the carbon monoxide conversion is

improved in the WGS bed. In addition, both methane conversion and carbon dioxide reduction increase with increasing steam-to-carbon ratio.

In this paper, the transport and chemical reaction in an industrial-scale steam methane reformer is simulated using CFD. The influence of burner on/off manners on the catalyst tube temperature and the hydrogen yield of an industrial-scale side-fired steam methane reformer is investigated. The aim is to seek a feasible burner on/off manner that has acceptable catalyst tube temperature and hydrogen yield, so as to improve the performance and service life of a steam methane reformer.

## 2. Numerical Methods and Physical Models

In this study, the ANSYS FLUENT V.17 commercial code [10] is employed to simulate the reacting and fluid flow in a steam methane reformer. The SIMPLE algorithm by Patankar [11] is used to solve the governing equations. The discretizations of convection terms and diffusion terms are carried out by the second-order upwind scheme and the central difference scheme, respectively. In respect to physical models, by considering the accuracy and stability of the models and by referring to the other CFD researches [3-5] of steam methane reformers, the standard  $k$ - $\varepsilon$  model [12], Discrete Ordinate (DO) radiation model [13] and Finite Rate/Eddy Dissipation (FRED) model [14] are adopted for turbulence, radiation and chemical reaction simulations, respectively. The standard wall functions [15] are used to resolve the flow quantities (velocity, temperature, and turbulence quantities) at the near-wall regions.

For the steady-state three-dimensional flow field with chemical reaction in this study, the governing equations include the continuity equation, momentum equation, turbulence model equation ( $k$ - $\varepsilon$  model), energy equation, radiation model equation (discrete ordinates radiation model), and chemical reaction model equation (FRED model). Among these models, only the FRED chemical reaction model is described below while the others and the convergence criterion are not described because they have been introduced in the author's previous study [16].

Consider the general form of the  $r^{\text{th}}$  chemical reaction as follows:



where

$N$  = number of chemical species in the system

$v'_{i,r}$  = stoichiometric coefficient for reactant  $i$  in reaction  $r$

$v''_{i,r}$  = stoichiometric coefficient for product  $i$  in reaction  $r$

$\mu_i$  = species  $i$

$k_{f,r}$  = forward rate constant for reaction  $r$

$k_{b,r}$  = backward rate constant for reaction  $r$

Eq. (4) is valid for both reversible and non-reversible reactions. For non-reversible reactions, the backward rate constant,  $k_{b,r}$ , is omitted. The species transport equation of a chemical reaction system can be written as

$$\nabla \cdot (\rho \bar{v} Y_i) = \nabla \cdot \left( \rho D_{i,m} + \frac{\mu_t}{Sc_i} \right) \nabla Y_i + R_i + S_i \quad (5)$$

where  $Y_i$ ,  $D_{i,m}$ ,  $Sc_i$ ,  $R_i$ , and  $S_i$  are the mass fraction, diffusion coefficient, turbulent Schmidt number, net generation rate, and extra source term of species  $i$ , respectively. The net source of chemical species  $i$  due to reaction is computed as the sum of the Arrhenius reaction sources over the  $N_R$  reactions that the species participate in  $\hat{R}$

$$R_i = M_{w,i} \sum_{r=1}^{N_R} \hat{R}_{i,r} \quad (6)$$

where  $M_{w,i}$  is the molecular weight of species  $i$  and  $\hat{R}_{i,r}$  is the Arrhenius molar rate of creation/destruction of species  $i$  in reaction  $r$ . For a non-reversible reaction, the molar rate of creation/destruction of species  $i$  in reaction  $r$  is given by

$$\hat{R}_{i,r} = \Gamma (v''_{i,r} - v'_{i,r}) \left( k_{f,r} \prod_{j=1}^N [C_{j,r}]^{\eta'_{j,r}} \right)^{(v'_{i,r} + \eta'_{i,r})} \quad (7)$$

For a reversible reaction,

$$\hat{R}_{i,r} = \Gamma (v''_{i,r} - v'_{i,r}) \left( k_{f,r} \prod_{j=1}^N [C_{j,r}]^{\eta'_{j,r}} - k_{b,r} \prod_{j=1}^N [C_{j,r}]^{v''_{j,r}} \right) \quad (8)$$

where

$C_{j,r}$  = molar concentration of species  $j$  in reaction  $r$  (kgmol/m<sup>3</sup>)

$\eta'_{j,r}$  = rate exponent for reactant species  $j$  in reaction  $r$

$\eta''_{j,r}$  = rate exponent for product species  $j$  in reaction  $r$

$\Gamma$  = net effect of third bodies on the reaction rate

The forward and backward rate constants for reaction  $r$ ,  $k_{f,r}$  and  $k_{b,r}$ , are computed using the Arrhenius expression:

$$k_{f,r} = A_r T^{\beta_r} e^{-E_r/RT} \quad (9)$$

$$k_{b,r} = \frac{k_{f,r}}{K_r} \quad (10)$$

where

$A_r$  = pre-exponential factor (consistent units)

$\beta_r$  = temperature exponent (dimensionless)

$E_r$  = activation energy for the reaction (J/kgmol)

$R$  = universal gas constant (J/kgmol-K)

$K_r$  is the equilibrium constant for the  $r^{\text{th}}$  reaction and is computed from

$$K_r = \exp \left( \frac{\Delta S_r^0}{R} - \frac{\Delta H_r^0}{RT} \right) \left( \frac{p_{atm}}{RT} \right)^{\sum_{i=1}^N (v''_{i,r} - v'_{i,r})} \quad (11)$$

where  $p_{atm}$  denotes atmospheric pressure (101, 325 Pa). The term within the exponential function represents the change in Gibbs free energy, and its components are computed as follows:

$$\frac{\Delta S_r^0}{R} = \sum_{i=1}^N (v''_{i,r} - v'_{i,r}) \frac{S_i^0}{R} \quad (12)$$

$$\frac{\Delta H_r^0}{RT} = \sum_{i=1}^N (v''_{i,r} - v'_{i,r}) \frac{h_i^0}{RT} \quad (13)$$

where  $S_i^0$  and  $h_i^0$  are the standard-state entropy and standard-state enthalpy (heat of formation). In this study, the kinetic and thermodynamic constants for reactions (1-3) used in Chibane and Djellouli's work [17] are adopted.

In general, a reformer operates at high temperatures. For a non-premixed reaction, turbulence mixes the reactants and then advects the mixture to the reaction zone for quick reaction. For a premixed reaction, turbulence mixes the lower-temperature reactants and the higher-temperature products and then advects the mixture to the reaction zone for a quick reaction. Therefore,

the chemical reaction is generally mixing (diffusion) controlled. However, the flue gas, fuel gas, and air are generally premixed before injecting into the reformer. Although the chemical reaction in most regions in a reformer is mixing controlled, in some regions, e.g., the neighborhood of the feed inlet, the chemical reaction is kinetically controlled. In existing chemical reaction models, the Eddy Dissipation Model (EDM) [18] can consider simultaneously the diffusion controlled and the kinetically controlled reaction rates. In EDM, the net generation rate of species  $i$  in the  $r^{\text{th}}$  chemical reaction is found from the smaller value of the following two reaction rates:

$$R_{i,r} = v'_{i,r} M_{w,i} A \rho \frac{\varepsilon}{k} \min_R \left( \frac{Y_R}{v'_{R,r} M_{w,R}} \right) \quad (14)$$

$$R_{i,r} = v'_{i,r} M_{w,i} A B \rho \frac{\varepsilon}{k} \frac{\sum_P Y_P}{\sum_j v''_{j,r} M_{w,j}} \quad (15)$$

where

$Y_p$  is the mass fraction of any product,  $P$

$Y_R$  is the mass fraction of a particular reactant,  $R$

$A$  is an empirical constant equal to 4.0

$B$  is an empirical constant equal to 0.5

In general, the EDM works well for a non-premixed reaction. However, for a premixed reaction, the reaction may start immediately when injecting into a reformer. This is unrealistic in practical situations. To overcome this unreasonable phenomenon, ANSYS FLUENT provides another model, the Finite-Rate/Eddy-Dissipation (FRED) model, which combines the finite-rate model and the EDM. In this model, the net generation rate of a species is taken as the smaller value of the Arrhenius reaction rate and the value determined by EDM. The Arrhenius reaction rate plays the role of a switch to avoid the unreasonable situation that the reaction starts immediately when injecting into a reformer. Once the reaction is activated, the eddy-dissipation rate is generally lower than the Arrhenius reaction rate, and the reaction rate is then determined by the EDM.

### 3. Results and Discussion

To validate the numerical methods and physical models used in this study, an industrial-scale steam methane reformer is simulated. The configuration and dimension of the reformer investigated are shown in Fig. 1. Note that only one half of the reformer is simulated due to its symmetry, as shown in Figure 1b,c. The reformer contains 138 reforming tubes and 216 burners on one side (totally 276 tubes and 432 burners). The outer diameter and thickness of a reforming tube are 136mm and 13.4 mm, respectively, while the diameter of a burner is 197 mm.

The boundary conditions for the numerical model of the steam methane reformer are described below. These conditions are practical operating conditions that are used by a petrochemical corporation in Taiwan.

- (1) Symmetry plane: symmetric boundary condition
- (2) Wall: standard wall function
- (3) Reforming tube inlet:

$$V = 5.4 \text{ m/s (in axial direction)}$$

$$T = 912.75 \text{ K}$$

$$P_{\text{gauge}} = 2.1658 \times 10^6 \text{ N/m}^2$$

Species mole fraction:

$$\text{CH}_4 = 0.2029$$

$$\text{H}_2\text{O} = 0.6$$

$$\text{H}_2 = 0.12855$$

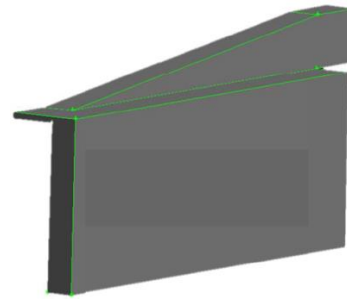
$$\text{CO}_2 = 0.06565$$

$$\text{CO} = 0.00145$$

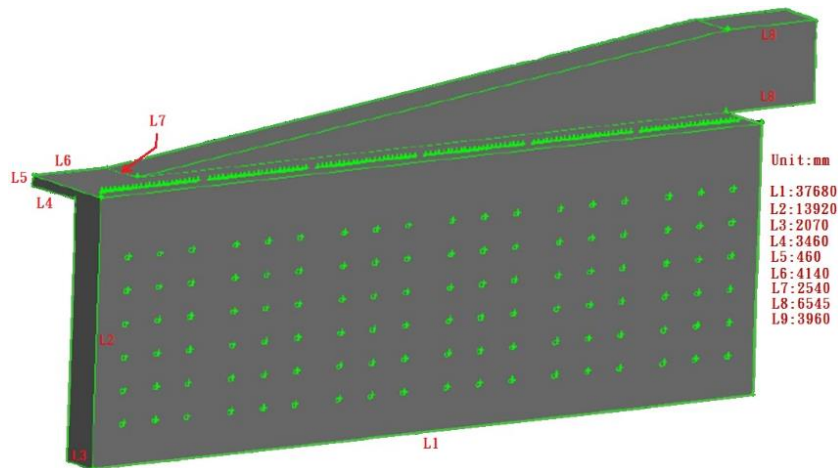
$$\text{N}_2 = 0.00145$$



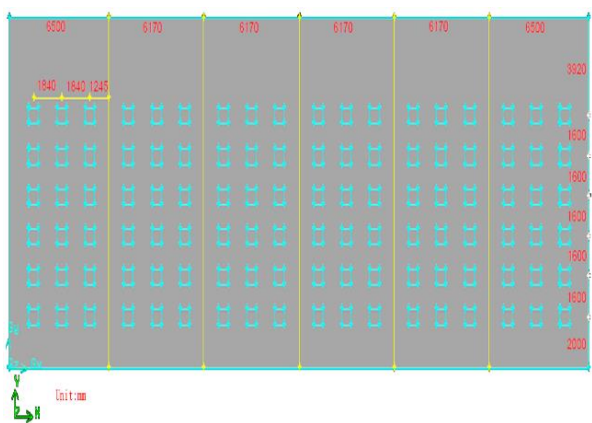
(a) A typical steam methane reformer



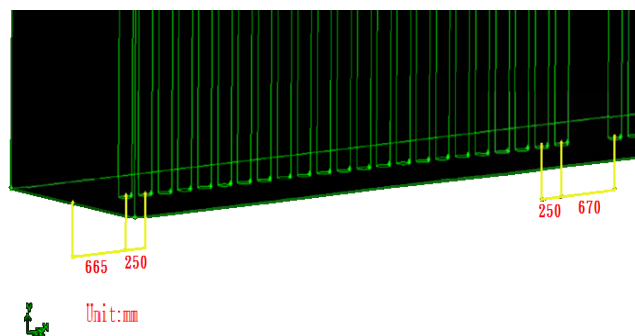
(b) A numerical model of the steam methane reformer



(c) The dimension of the steam methane reformer



(d) Illustration of the burner positions



(e) Illustration of the reforming tube positions

Fig. 1 Configuration and dimension of the steam methane reformer investigated

(4) Reforming tube exit

The diffusion flux for all flow variables in the outflow direction are zero. In addition, the mass conservation is obeyed at the exit.

(5) Fuel and flue gas inlet (burner inlet):

$$V = 2.404 \text{ m/s (in radial direction)}$$

$$T = 673.15 \text{ K}$$

$$P_{\text{gauge}} = 1.04544 \times 10^4 \text{ N/m}^2$$

Species mole fraction:

$$H_2 = 0.0816$$

$$CH_4 = 0.0474$$

$$N_2 = 0.49057$$

$$O_2 = 0.12818$$

$$CO_2 = 0.25225$$

(6) Fuel and flue gas exit:

The diffusion flux for all flow variables in the outflow direction are zero. In addition, the mass conservation is obeyed at the exit.

The turbulence kinetic energy is 10% of the inlet mean flow kinetic energy and the turbulence dissipation rate is computed using Eq. (16).

$$\varepsilon = C_{\mu}^{3/4} \frac{k^{3/2}}{l} \quad (16)$$

where  $l = 0.07 L$  and  $L$  is the hydraulic diameter.

### 3.1. Comparison of numerical results with experimental data

The simulation results are compared with the experimental data from a petrochemical refinery in Taiwan to evaluate the numerical methods and physical models adopted in this study. The temperature of the reformer is detected by an Infrared thermographer with radiation emissivity of 0.92, the Field Of View (FOV) 24mm and object distance of 5m.

As mentioned above, the real reformer contains 138 reforming tubes and 216 burners on one side (totally 276 tubes and 432 burners). To save simulation time, a simplified model is also calculated and compared. The simplified model contains 6 tubes and 12 burners on one side of the reformer. The arrangement of reforming tubes and burners as well as their dimensions for the simplified model is shown in Fig. 2. The flow rates in the reforming tubes and burners for the simplified model are the same as those in the real reformer. Therefore, the reforming tubes and burners for the simplified model have larger diameters.

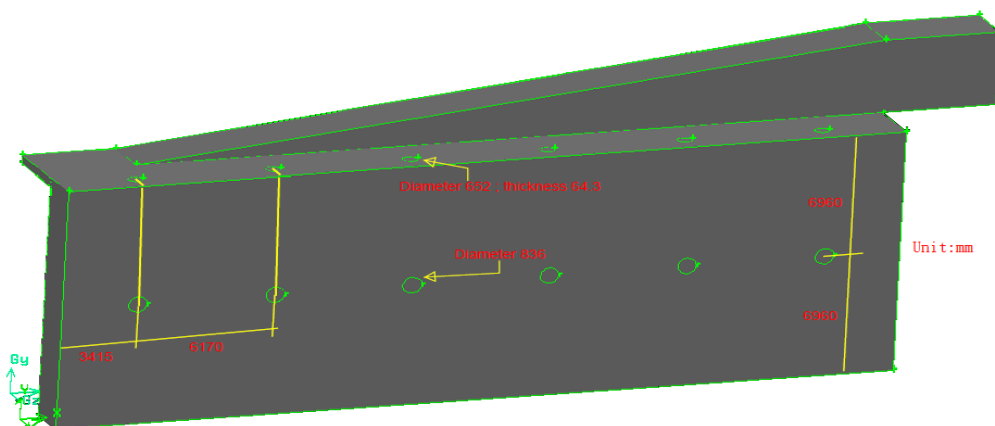


Fig. 2 The arrangement of reforming tubes and burners as well as their dimensions for the simplified model

The computer used in this study is an ASUS ESC-500-G4 work station of 8 cores with Intel Core i7-6700 CPU and 64 GB ram. The numbers of CFD cells for the real reformer model and the simplified model are around 4 million and 1.5 million, respectively. The grid mesh is generated by the software GAMBIT and is unstructured. The dimensionless distance from the wall,  $y^*$ , in the wall function method has been examined after a converged solution is obtained. It was found that the values of  $y^*$  for the nodes at the wall to their nearest interior nodes vary between 20.0 and 60.0, and lie in the logarithmic layer of the wall function method. This implies that the wall-adjacent cells of the grid mesh in this study are suitable for the use of wall function. The solution of the CFD model for the real reformer is obtained after approximately 30 full days while that for the simplified reformer is approximately 10 full days.

Fig. 3 compares the average temperatures at the outer surfaces of the reforming tubes. It can be seen that the simulation result agrees well with the experimental data. The deviations from the experimental data using the real reformer model and the simplified model are 2.88% and 3.18%, respectively, which are both acceptable from a viewpoint of engineering applications. The result calculated from the real reformer model agrees better with the experimental data than that from the simplified model, although the latter also gives an acceptable result.

Fig. 4 shows the simulated hydrogen yield at the reforming tube outlets using a simplified model. The experimental value of the hydrogen yield is 0.698. The simulated value is 0.708. The deviation of the CFD simulation is 1.43%.

In the subsequent discussion, the simplified model is used for the parametric study to save simulation time.

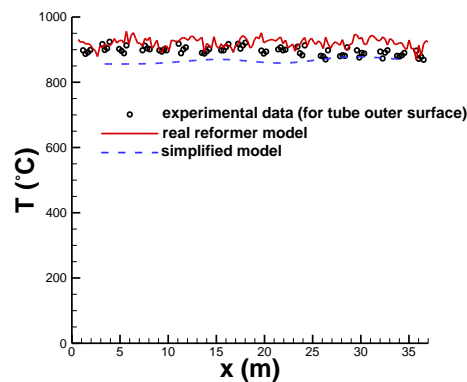


Fig. 3 Comparison of the average temperatures at the outer surfaces of the reforming tubes

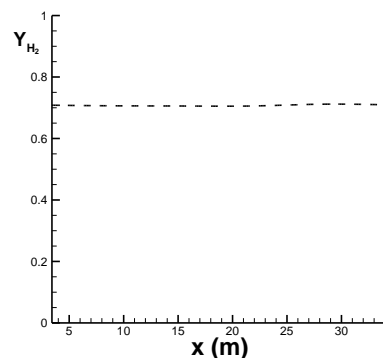


Fig. 4 The simulated average mole fraction of hydrogen at the reforming tube outlets

### 3.2. Effect of the burner on/off manner

To explore the effect of the burner on/off manner on the thermal field and hydrogen yield, the burners are divided into six groups. The first group ranges from  $x=0$  to  $x=6.5$ m, the second group ranges from  $x=6.5$  to  $x=12.67$ m, the third group ranges from  $x=12.67$  to  $x=18.84$ m, the fourth group ranges from  $x=18.84$  to  $x=25.01$ m, the fifth group ranges from  $x=25.01$  to  $x=31.18$ m, and the sixth group ranges from  $x=31.18$  to  $x=37.68$ m. Each group of burners can be controlled on or off. In the following discussion, 12 different manners of the burner on/off are discussed.

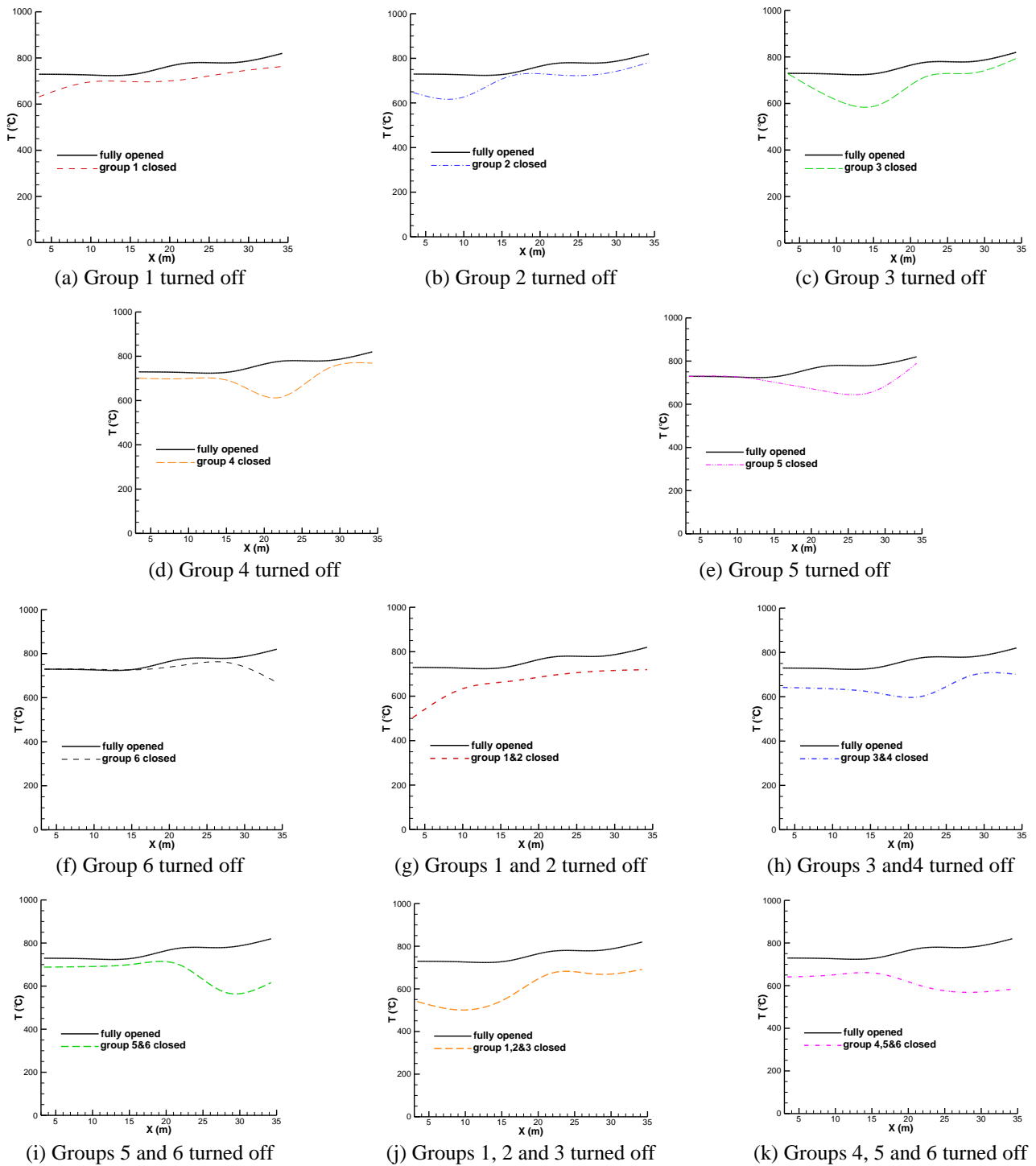


Fig. 5 Comparison of the average temperatures at the outer surfaces of the reforming tubes

Fig. 5 and 6 compare the average temperatures at the inner and outer surfaces, respectively, of the reforming tubes using different manners of the burner on/off. From the simulation results, it is seen that temperature profiles are obviously influenced by the manners of the burner on/off. When one group of burners is turned off, the outer surface temperatures of the tubes are decreased by about 94°C on average, and the inner surface temperatures are decreased by about 54°C on average. When two groups of burners are turned off, the outer surface temperatures of the tubes are decreased by about 175°C on average, and the inner surface temperatures are decreased by about 106°C on average. When three groups of burners are turned off, the outer surface temperatures of the tubes are decreased by about 251°C on average, and the inner surface temperatures are decreased by about 151°C on average. The tube temperatures reduce in regions where burners are turned off. When the central groups of burners are turned off, the tube temperatures have greater reductions. On the other hand, when the rear groups of burners are turned off, the tube temperatures have lower reductions. The results can also be observed in Table 1.

For a reformer operating at a high temperature, the heat transfer to the catalyst tubes comes primarily from the radiation of the fired walls and the combustion gas, and secondarily from the convection of the combustion gas. In terms of radiation, the radiation intensity from the middle groups of burners is higher than that from the side groups of burners. This is because the view factors among the middle groups of burners and the reformer tubes are larger than those among the side groups of burners and the reformer tubes. In terms of convection, turning off the upstream groups of burners can alleviate convection to the downstream region and hence can reduce the tube temperature to a higher extent. On the contrary, turning off the downstream groups of burners has little influence on the convection to the upstream region and hence can reduce the tube temperature only to a lower extent.

Table 1 Comparison of the average temperatures at the reforming tube surface

operating manner of the burners	the average temperature of tube outer surfaces ( $^{\circ}\text{C}$ )	the average temperature of tube inner surfaces ( $^{\circ}\text{C}$ )
fully opened	866	761
group 1 turned off	770	706
group 2 turned off	769	704
group 3 turned off	767	697
group 4 turned off	768	701
group 5 turned off	776	710
group 6 turned off	780	727
group 1&2 turned off	690	654
group 3&4 turned off	684	649
group 5&6 turned off	699	661
group 1,2&3 turned off	609	605
group 4,5&6 turned off	621	616

The above result can also be observed from Fig. 7 which compares the average mole fractions of hydrogen at the reforming tube outlets using different manners of the burner on/off. It can be found from Fig. 7 that the simulated hydrogen yield is 0.708 for the case of burners fully opened. The real value of the hydrogen yield is 0.698. The deviation of the CFD simulation is 1.43%. It is also observed that the hydrogen yields reduce in regions where burners are turned off. The more the burners are turned off, the greater the reduction in hydrogen yields will be. Table 2 shows the comparison of the average mole fractions of hydrogen at the reforming tube outlets using different manners of the burner on/off. It is observed that when one group of burners is turned off, the hydrogen yields are decreased by about 4%. When two groups of burners are turned off, the hydrogen yields are decreased by about 7.9%. When three groups of burners are turned off, the hydrogen yields are decreased by about 11.4%. When the central groups of burners are turned off, the hydrogen yields have greater reductions. On the other hand, when the rear groups of burners are turned off, the hydrogen yields have lower reductions.

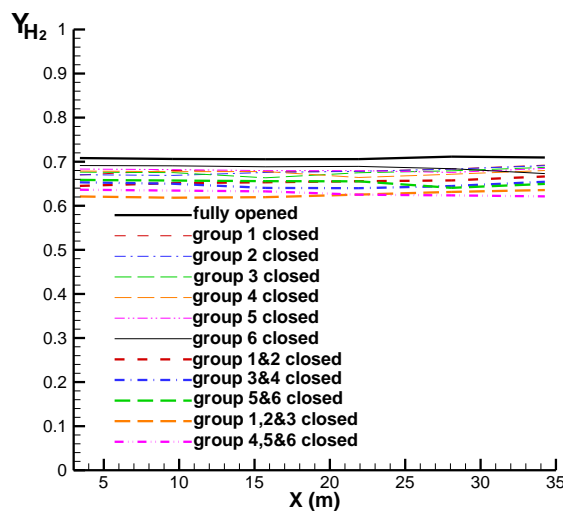


Fig. 6 Comparison of the average mole fractions of hydrogen at the reforming tube outlets

Table 2 Comparison of the average mole fractions of hydrogen at the reforming tube outlets

operating manner	average mole fractions of hydrogen at the reforming tube outlets
fully opened	0.708
group 1 turned off	0.681
group 2 turned off	0.678
group 3 turned off	0.676
group 4 turned off	0.675
group 5 turned off	0.681
group 6 turned off	0.686
group 1&2 turned off	0.655
group 3&4 turned off	0.647
group 5&6 turned off	0.653
group 1,2&3 turned off	0.625
group 4,5&6 turned off	0.629

#### 4. Conclusions

In this research, the effect of the burner on/off manners on an industrial-scale side-fired steam methane reformer is investigated to seek a feasible burner on/off manner that has acceptable catalyst tube temperature and hydrogen yield, so as to improve the performance and service life of a steam methane reformer. It is found that when one group of burners is turned off, the outer surface temperatures of the tubes are decreased by about 94°C in average, the inner surface temperatures are decreased by about 54°C in average, and the hydrogen yields are decreased by about 4%. When two groups of burners are turned off, the outer surface temperatures of the tubes are decreased by about 175°C in average, the inner surface temperatures are decreased by about 106°C in average, and the hydrogen yields are decreased by about 7.9%. When three groups of burners are turned off, the outer surface temperatures of the tubes are decreased by about 251°C in average, the inner surface temperatures are decreased by about 151°C in average, and the hydrogen yields are decreased by about 11.4%. The tube temperatures and the hydrogen yields reduce to a greater extent in regions where burners are turned off. When the central groups of burners are turned off, the tube temperatures and the hydrogen yields have greater reductions. On the other hand, when the rear groups of burners are turned off, the tube temperatures and the hydrogen yields have lower reductions. The result of this paper is helpful in improving the performance and service life of a steam methane reformer.

#### Funfing

This research and the APC were funded by the Ministry of Science and Technology, Taiwan, under the contract MOST107-2221-E-150-061.

#### Acknowledgement

The author is grateful to the Formosa Petrochemical Corporation in Taiwan for providing valuable data and constructive suggestions to this research during the execution of the industry-university cooperative research project under the contract 104AF-86.

#### Conflicts of Interest

The author declares no conflict of interest.

#### Abbreviations

The following abbreviations are used in this manuscript:

- $C_\mu$       turbulence model constant (=0.09)  
 $K$         turbulence kinetic energy ( $m^2/s^2$ )

P	pressure (N/m <sup>2</sup> )
T	temperature (K)
V	velocity (m/s)
XYZ	cartesian coordinates with origin at the centroid of the burner inlet (m)
Y	mole fraction (%)
Greek symbols	
$\varepsilon$	turbulence dissipation rate (m <sup>2</sup> /s <sup>3</sup> )
$\mu$	viscosity (kg/(m s))
$\rho$	density (kg/m <sup>3</sup> )
$\tau$	shear stress (N/m <sup>2</sup> )

## References

- [1] A. S. Kimmel, "Heat and mass transfer correlations for steam methane reforming in non-adiabatic, process-intensified catalytic reactors," Master thesis, Marquette University, Milwaukee, WI, USA, 2011.
- [2] L. Castagnola, G. Lomonaco, and R. Marotta, "Nuclear systems for hydrogen production: State of art and perspectives in transport sector," *Global Journal of Energy Technology Research Updates*, vol. 1, pp. 4-18, 2014.
- [3] A. Tran, A. Aguirre, H. Durand, M. Crose, and P. D. Christofides, "CFD modeling of an industrial-scale steam methane reforming furnace," *Chemical Engineering Science*, vol. 171, pp. 576-598, 2017.
- [4] A. Di Carlo, I. Aloisi, N. Jand, S. Stendardo, and P. U. Foscolo, "Sorption enhanced steam methane reforming on catalyst-sorbent bifunctional particles: A CFD fluidized bed reactor model," *Chemical Engineering Science*, vol. 173, pp. 428-442, 2017.
- [5] L. Lao, A. Aguirre, A. Tran, Z. Wu, H. Durand, and P. D. Christofides, "CFD modeling and control of a steam methane reforming reactor," *Chemical Engineering Science*, vol. 148, pp. 78-92, 2017.
- [6] E. M. A. Mokheimer, M. I. Hussain, S. Ahmed, M. A. Habib, and A. A. Al-Qutub, "On the modeling of steam methane reforming," *Journal of Energy Resources Technology*, vol. 137, 012001, 2015.
- [7] M. Ni, "2D heat and mass transfer modeling of methane steam reforming for hydrogen production in a compact reformer," *Energy Conversion and Management*, vol. 65, pp. 155-163, 2013.
- [8] H. Ebrahimi, J. S. Soltan Mohammadzadeh, A. Zamaniyan, and F. Shayegh, "Effect of design parameters on performance of a top fired natural gas reformer," *Applied Thermal Engineering*, vol. 28, pp. 2203-2211, 2008.
- [9] Y. S. Seo, D. J. Seo, Y. T. Seo, and W. L. Yoon, "Investigation of the characteristics of a compact steam reformer integrated with a water-gas shift reactor," *Journal of Power Sources* vol. 161, pp. 1208-1216, 2006.
- [10] Fluent Inc., ANSYS FLUENT 17 User's Guide, New York: Fluent Inc., 2017.
- [11] S. V. Patankar, *Numerical heat transfer and fluid flows*, New York: McGraw-Hill, 1980.
- [12] B. E. Launder and D. B. Spalding, *Lectures in mathematical models of turbulence*, London: Academic press, 1972.
- [13] R. Siegel and J. R. Howell, *Thermal radiation heat transfer*, Washington, DC: Hemisphere publishing corporation, 1992.
- [14] Y. R. Sivathanu and G. M. Faeth, "Generalized state relationships for scalar properties in non-premixed hydrocarbon/air flames," *Combustion and Flame*, vol. 82, pp. 211-230, 1990.
- [15] B. E. Launder and D. B. Spalding, "The numerical computation of turbulent flows," *Computer Methods in Applied Mechanics and Engineering*, vol. 3, pp. 269-289, 1974.
- [16] C. L. Yeh, "Numerical analysis of the combustion and fluid flow in a carbon monoxide boiler," *International Journal of Heat and Mass Transfer*, vol. 59, pp. 172-190, 2013.
- [17] L. Chibane and B. Djellouli, "Methane steam reforming reaction behaviour in a packed bed membrane reactor," *International Journal of Chemical Engineering and Applications*, vol. 2, pp. 147-156, 2011.
- [18] B. F. Magnussen and B. H. Hjertager, "On mathematical models of turbulent combustion with special emphasis on soot formation and combustion," *Proc. Symp. (international) on Combustion*, The Combustion Institute, 1976.

